

# Nonlinear ultrasonic parameter in quenched martensitic steels

D. C. Hurley,<sup>a)</sup> D. Balzar, P. T. Purtscher, and K. W. Hollman  
*National Institute of Standards & Technology, 325 Broadway, Boulder, Colorado 80303*

(Received 5 December 1997; accepted for publication 22 January 1998)

We have determined the nonlinear ultrasonic parameter  $\beta$  and the ultrasonic longitudinal phase velocity  $v_L$  for a series of martensitic steel specimens which varied in carbon content. The specimens were measured in the as-quenched state to ensure that the carbon was present primarily as an interstitial in the martensite.  $\beta$  increased monotonically with carbon content and hardness over the range 0.10–0.40 mass % C (39.0–57.5 Rockwell C hardness). However,  $v_L$  remained virtually the same for all specimens. Therefore we conclude that  $\beta$  is sensitive to microstructural variations between the specimens, but  $v_L$  is not. X-ray diffraction experiments indicate that the dislocation density in the specimens is large ( $\sim 10^{11}$ – $10^{12}/\text{cm}^2$ ) and increases with increasing carbon content. These results support the hypothesis that the observed increase in  $\beta$  can be attributed to dislocation-related effects in the specimens. [S0021-8979(98)01009-3]

## I. INTRODUCTION

In past decades, nonlinear ultrasonic techniques have been used most commonly to determine the third-order elastic moduli of single crystals (for reviews see Refs. 1 and 2). Interest in nonlinear ultrasonics in recent years, however, has focused mainly on its applications for engineering materials. For example, nonlinear ultrasonic properties have been found to correlate strongly with mechanical properties such as adhesion of composites,<sup>3</sup> precipitate hardening in aluminum,<sup>4</sup> and diffusion bond integrity in copper.<sup>5</sup> Much work remains before the full potential of nonlinear ultrasonic methods is fully understood and exploited for such uses. In this paper, we present results of nonlinear ultrasonic experiments on another material with industrial applications: martensitic steels. It is shown that the nonlinear parameter  $\beta$  depends strongly on the presence of dislocations in the quenched material.

## II. SPECIMEN PREPARATION

Using three types of steel (9310, 4320, and 4340), we fabricated specimens in which the mass percent of carbon varied from 0.10% to 0.40%. The carbon content of each specimen, determined by optical emission spectroscopy, is listed in Table I along with other specimen characteristics. Specimens ranged in cross section from 30×30 to 60×60 mm and were approximately 19 mm thick. The specimens were prepared by “soaking” them at about 100 °C above their critical temperature, that is, the temperature at which ferrite first begins to form from austenite upon cooling. The specimens were soaked for 1 h and then rapidly quenched to room temperature by immersion in an agitated water bath with a cooling rate of approximately 100 °C/s. This process was intended to achieve a martensitic microstructure in which the chief difference was the variation in amount of interstitial carbon. Measurements were performed on the specimens in the resulting as-quenched state, without addi-

tional tempering. The specimens were stored at room temperature during the measurement period (roughly 1 month).

Specimen microstructure was examined using a light microscope at 1000× magnification. The micrographs are shown in Fig. 1. They reveal that all three specimens possessed a uniform lath martensite structure. The average martensite packet length varied from specimen to specimen, but was within the range from 5 to 20  $\mu\text{m}$  for all specimens. The micrographs also indicate little or no evidence of retained austenite or second-phase formation.

The Rockwell C hardness (HRC) was determined for the quenched specimens. Each specimen was cut, and measurements were made at several locations along the thickness dimension. The average hardness of a specimen was then computed from this set of measurements. Since individual values varied by only the measurement uncertainty ( $\pm 1$  HRC), we concluded that the hardness of each specimen was uniform. The values in Table I show that the hardness ranged from 39.0 HRC to 57.5 HRC. A plot of hardness as a function of mass percent carbon, shown in Fig. 2, reveals that the hardness increased monotonically with carbon content over the range studied.

## III. ULTRASONIC PROPERTIES

### A. Longitudinal velocity

The longitudinal phase velocity  $v_L$  was measured in each specimen using an immersion, pulse-echo superposition technique<sup>6,7</sup> with an uncertainty of  $\pm 0.1\%$ . The experimen-

TABLE I. Properties of as-quenched steel specimens used in this work.

Steel	Mass % C	Soaking temperature (°C)	Hardness (HRC)
9310	0.10	900	39.0±1
4320	0.18	885	43.5±1
4340	0.40	870	57.5±1

<sup>a)</sup>Electronic mail: hurley@boulder.nist.gov

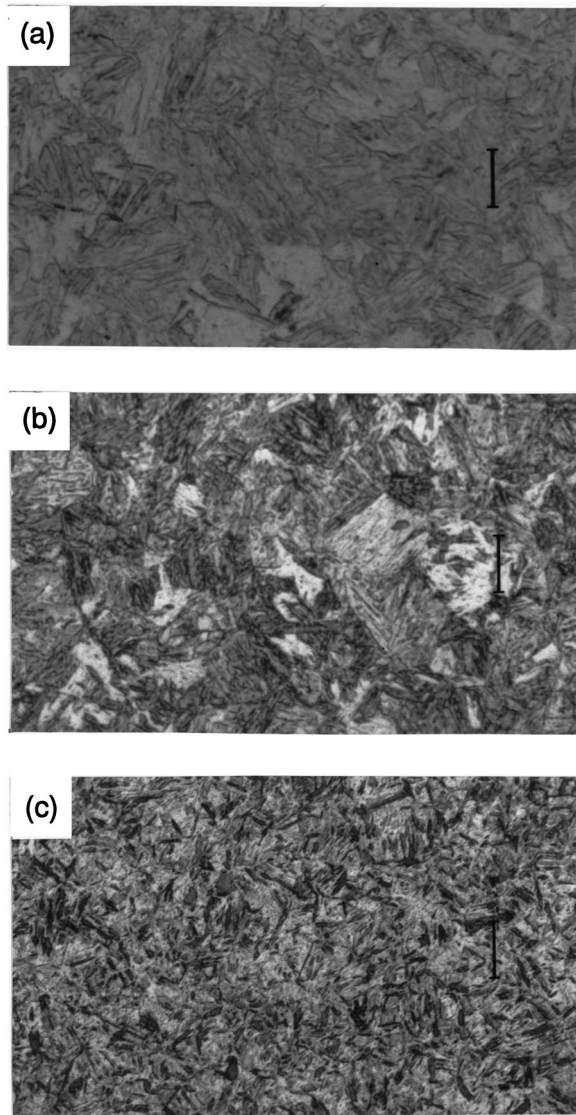


FIG. 1. Optical micrographs of quenched steel specimens (1000× magnification). The scale is indicated by the vertical black line in each photograph, which corresponds to 10 μm. (a) 9310 steel (0.10% C), (b) 4320 steel (0.18% C), (c) 4340 steel (0.40% C).

tal values for  $v_L$  in the as-quenched specimens are given in Table II and plotted in Fig. 3(a). Table II also indicates the velocity values relative to that for the 9310 (0.10% C) specimen. The graph reveals that  $v_L$  was nearly identical for all

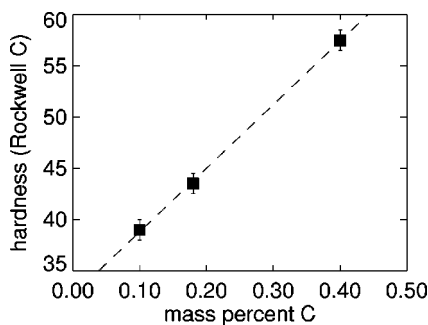


FIG. 2. Rockwell hardness as a function of nominal carbon content for the as-quenched specimens. The broken line is a linear least-squares fit.

TABLE II. Ultrasonic results for quenched steel specimens. Values for  $v_L$  and  $\beta$  for each specimen are expressed relative to the values  $v_L^0$  and  $\beta^0$  for the 9310 steel specimen.

Steel	Mass % C	$v_L$ (m/s)	$v_L/v_L^0$	$\beta$	$\beta/\beta^0$
9310	0.10	$5853 \pm 6$	1	$5.49 \pm 0.33$	1
4320	0.18	$5874 \pm 6$	$1.004 \pm 0.001$	$5.71 \pm 0.34$	$1.04 \pm 0.02$
4340	0.40	$5855 \pm 6$	$1.000 \pm 0.001$	$6.12 \pm 0.37$	$1.11 \pm 0.02$

specimens. Minor differences in velocity slightly larger than the experimental uncertainty were measured, but no consistent trend was observed.

### B. Nonlinear ultrasonic parameter

The nonlinear ultrasonic parameter  $\beta$  for each of these specimens was determined through harmonic-generation experiments.<sup>2,8</sup> In the experiments, longitudinal tonebursts at the fundamental angular frequency  $\omega_0 = 2\pi \times 9.8$  MHz were generated by a piezoelectric transducer bonded to one side of the specimen. The transmitted ultrasonic waves detected on the other side of the specimen contained a displacement component of amplitude  $A_1$  at  $\omega_0$ , a component of amplitude  $A_2$  at the second-harmonic frequency  $2\omega_0$ , and so on. The waveforms were detected using a path-stabilized Michelson interferometer (laser wavelength  $\lambda = 1064$  nm). Our interferometric detection techniques have been described in detail elsewhere.<sup>8</sup> Michelson interferometry provides a straightforward means to measure the fundamental and harmonic components, since the absolute ultrasonic displacements are re-

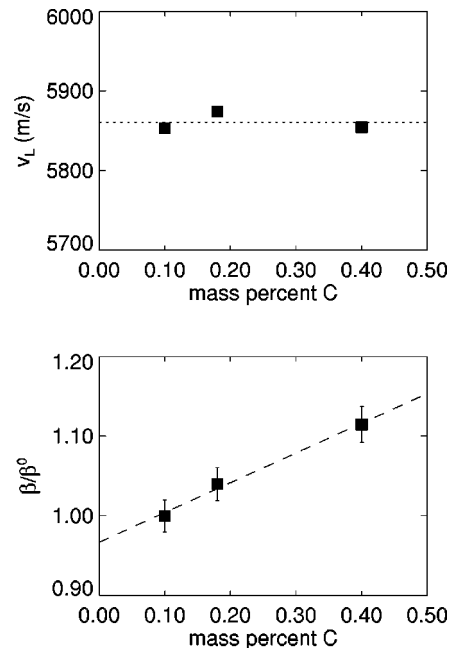


FIG. 3. (a) Longitudinal ultrasonic velocity  $v_L$  as a function of carbon content for the quenched steel specimens. The uncertainty in velocity ( $\pm 6$  m/s) is smaller than the plotting symbol. The dotted line indicates the average velocity ( $v_L = 5861$  m/s) of all three specimens. (b) Nonlinear ultrasonic parameter  $\beta$  for the same specimens. The data are normalized to the value of  $\beta$  for the 9310 specimen ( $\beta^0 = 5.49 \pm 0.33$ ). The broken line represents a linear least-squares fit to the data.

lated directly to the accurately known laser wavelength. The detected waveforms were digitally processed using simple frequency-notch filters to obtain the displacement amplitudes  $A_1$  and  $A_2$ .

Given the fundamental and second-harmonic amplitudes, the magnitude of the nonlinear parameter  $\beta$  was determined through the relationship<sup>2</sup>

$$|\beta| = \frac{8v_L^2 A_2}{\omega_0^2 z A_1^2}, \quad (1)$$

where  $z$  is the specimen thickness. For each specimen, several amplitude pairs ( $A_1$ ,  $A_2$ ) were obtained using stepped attenuators to vary the input power. Typically,  $A_1 \approx 2\text{--}6$  nm. The least-squares-fit slope of the line  $A_2$  vs  $A_1^2$  was then calculated and used with Eq. (1) to obtain the value for  $|\beta|$  in the specimen. Next, a correction factor that accounted for diffraction of the fundamental and second-harmonic waves<sup>8</sup> was calculated for each specimen. The experimental values were multiplied by these factors to obtain the final values of  $|\beta|$ .

The experimentally determined values of  $|\beta|$  are given in Table II. (For ease of notation, we will refer to  $|\beta|$  simply as  $\beta$  throughout the rest of this paper.) The absolute values of  $\beta$  possessed an estimated uncertainty of  $\pm 6\%$ . A large portion of the uncertainty originated from common sources such as oscilloscope gain. Therefore, it was possible to reduce the experimental uncertainty to  $\pm 2\%$  for a series of specimens by expressing  $\beta$  in terms of relative values. Table II shows the values of  $\beta$  relative to the value  $\beta^0$  for the 9310 steel specimen.

The relative values for  $\beta$  are plotted versus carbon content in Fig. 3(b). The graph reveals that  $\beta$  varied significantly from specimen to specimen, even though the uncertainty for  $\beta$  was over ten times larger than that for  $v_L$ . Furthermore,  $\beta$  increased monotonically with carbon content. For example, an increase in  $\beta$  of 11% from the 0.10% C to the 0.40% C specimen was measured. Comparison of Figs. 3(a) and 3(b) makes it clear that  $\beta$  is much more sensitive to microstructural differences between the specimens than is  $v_L$ .

Strictly speaking, Eq. (1) should include a correction factor<sup>9</sup> to account for ultrasonic attenuation of the fundamental and second harmonic components. Attenuation measurements were not performed on these specimens. However, previous studies in quenched martensite<sup>10,11</sup> suggest that attenuation corrections should increase the absolute values of  $\beta$  by only a few percent at most. Moreover, assuming that the attenuation is approximately the same for all specimens, the relative values of  $\beta$  would remain nearly unchanged.

#### IV. X-RAY DIFFRACTION EXPERIMENTS

To obtain further microstructural information, x-ray diffraction experiments were performed on the specimens. Diffraction line-broadening analysis<sup>12</sup> can be used to quantify structural defects related to both size (stacking and twin faults, low-angle and high-angle boundaries) and strain (dislocations and point defects) effects. Observed x-ray diffraction patterns were modeled with a Rietveld-refinement program.<sup>13,14</sup>

TABLE III. X-ray diffraction results for quenched steel specimens.

Steel	Mass % C	$\epsilon$ ( $10^{-3}$ )	$N$ ( $10^{11}/\text{cm}^2$ )
9310	0.10	$3.0 \pm 0.2$	$6.1 \pm 0.6$
4320	0.18	$3.3 \pm 0.2$	$7.8 \pm 0.8$
4340	0.40	$4.6 \pm 0.6$	$15 \pm 4$

Preliminary diffraction-line-broadening analysis indicated an insignificant anisotropy effect, and only the isotropic line-broadening parameters were refined using the Rietveld program. Results showed that size-related effects caused negligible broadening. (The estimated minimum size of coherently diffracting domains was approximately 300 nm.) This fact confirmed that transformation twinning in the specimens was negligible, as expected for pure lath martensite. Therefore, we concluded that all broadening was strain-related. Using the full width at half maximum of the refined diffraction line and correcting for instrumental line broadening,<sup>15</sup> we estimated the strain  $\epsilon$  for each specimen. Table III shows that values for  $\epsilon$  were relatively large—in the range  $3\text{--}5 \times 10^{-3}$ .

There are two possible sources of strain-related line broadening in martensite: interstitial carbon atoms and dislocations. In an isotropic, elastic-continuum misfit-sphere approximation,<sup>16</sup> carbon atoms cause an overall expansion of the host lattice. In addition, the distortion of the host lattice in the vicinity of the carbon atoms produces an inhomogeneous (local) strain that contributes to the diffraction line broadening. However, we think that the contribution from interstitial strain is relatively small in our specimens for several reasons. First, the concentration of interstitials is relatively low in these steels. Second, the radial component of strain decreases as the third power of distance from the carbon atom,<sup>17</sup> so the effect is highly localized. Third, similar effects in Al-Si alloys are small.<sup>18</sup> Therefore the contribution of interstitial strain is thought to be relatively small and masked by dislocation-related strain effects, which are substantially greater.

High dislocation densities are expected in lath martensite, since the Bain distortion is accompanied by dislocation slip that relieves the transformation strain.<sup>19</sup> The dislocation slip is along  $\{111\}$  fcc planes, which is equivalent to  $\{011\}$  bcc slip shear. In the isotropic approximation, neglecting possible interactions between pure screw dislocations, the dislocation density  $N$  is given by<sup>20</sup>

$$N = k \frac{\epsilon^2}{b^2}. \quad (2)$$

Here  $\epsilon$  is the strain calculated from diffraction line broadening, and the constant  $k = 14.4$  assuming<sup>17</sup> that the Burgers vector  $\mathbf{b} = a/2 [111]$ .

The values for  $N$  calculated from Eq. (2) are given in Table III and are plotted as a function of carbon content in Fig. 4. For these specimens,  $N$  was in the range  $6\text{--}15 \times 10^{11}/\text{cm}^2$ . This is consistent with typical estimates of  $N \approx 10^{11}\text{--}10^{12}/\text{cm}^2$  in quenched martensite.<sup>21</sup> Equation (2) gives an upper limit for  $N$ , since the line broadening due to

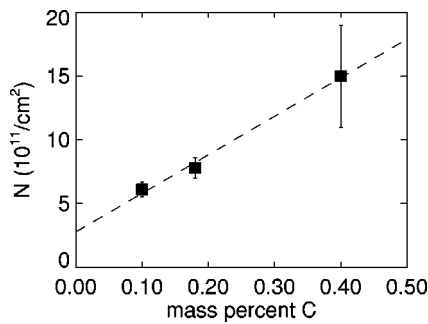


FIG. 4. Dislocation density  $N$  in the specimens obtained from x-ray diffraction line-broadening experiments. A linear least-squares fit to the data is indicated by the broken line.

local strain variations by interstitial carbon was neglected. Moreover, some dislocation pileup is expected due to the high dislocation density. Nevertheless, Fig. 4 shows that  $N$  increases monotonically with carbon content in the specimens. This behavior is expected from the mechanism of Bain transformation and is in agreement with previous experiments.<sup>22</sup>

## V. DISCUSSION OF RESULTS

Examination of Figs. 3(b) and 4 suggests a relationship between  $\beta$  and  $N$ , since both exhibit a correlation with carbon content. This is confirmed in Fig. 5, which shows the values of  $\beta$  obtained in harmonic-generation experiments versus the x-ray diffraction values for  $N$ . The figure clearly indicates that  $\beta$  increases monotonically with the dislocation density  $N$ .

Insight into this relationship can be found by examination of previous work on harmonic generation by dislocations. Hikata and co-workers<sup>23,24</sup> showed that in single-crystal aluminum, second-harmonic generation was very sensitive to dislocations acted upon by applied or internal stresses. Although initial experiments investigated the effect of external (applied) stresses on harmonic generation,<sup>23</sup> later experiments<sup>24</sup> showed that internal stresses created by plastic deformation produced similar effects.

The experimental results of Hikata *et al.* were interpreted using a model for second-harmonic generation of longitudinal waves by bowed-out dislocations.<sup>25,26</sup> The model assumed a network of dislocations of density  $N$  and loop length  $L$ , acting under an applied stress  $\sigma$ . With these as-

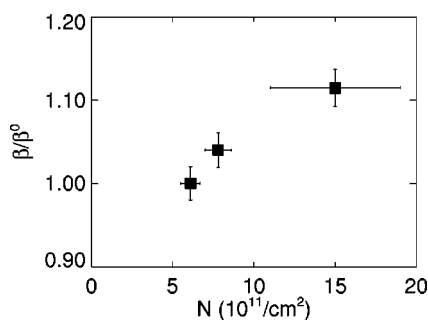


FIG. 5. Normalized nonlinear parameter  $\beta$  vs dislocation density  $N$  determined from x-ray diffraction experiments.

sumptions, nonlinear terms were added to the Granato–Lücke theory of pinned dislocations,<sup>27</sup> and equations were derived to predict the amplitude of the second harmonic. In terms of the nonlinear parameter  $\beta$ , the model predicted a dislocation contribution to  $\beta$  that was linear in both  $N$  and  $\sigma$  and depended on the fourth power of  $L$ :  $\beta \propto NL^4\sigma$ .

We think that this mechanism, namely harmonic generation by dislocations under stress, can be used to interpret our results. The quenched lath martensite specimens contain internal stresses associated with very large dislocation densities and interstitial carbon. The dislocation networks produce long-range internal stress fields which are particularly strong close to the dislocation core. Coupled with the locally high strain fields of interstitial carbon atoms, these internal stresses create an asymmetric, nonlinear stress-strain relation in the vicinity of the dislocations. It is this asymmetry that enables second-harmonic generation by dislocations.<sup>25</sup>

Existing theory<sup>25,26</sup> does not encompass many features of the quenched steel system. For instance, the theory considered only the case of uniaxial applied stress in single crystals. Several simplifying assumptions were also made. For example, a single loop length  $L$  was used to describe the system, which is clearly not appropriate to the steel specimens. The theory can therefore be used only for qualitative interpretation of our results. With this in mind, we find that the monotonic increase in  $\beta$  with  $N$  indicated in Fig. 5 roughly agrees with the linear relationship predicted by the theory. Furthermore, the theory can be used to calculate the approximate magnitude of the effect. With realistic values of dislocation and material parameters in the steels, our order-of-magnitude estimates based on the equations of Hikata *et al.* indicate that dislocation–stress interactions could produce sufficient second harmonics to increase  $\beta$  by observed amounts. Therefore, we think that our results are consistent with the model of Hikata *et al.* for second-harmonic generation by dislocations under stress.

Further work is needed to develop a more systematic understanding of the microstructural mechanisms which account for the observed behavior. More complete understanding requires more specimens with a greater variety of carbon content. With additional specimens, the functional dependence of  $\beta$  on  $N$  could be better determined. Moreover, as noted by previous authors, it is difficult to use longitudinal second-harmonic generation measurements to interpret dislocation behavior in greater detail than the semiquantitative nature discussed above. The lattice contribution and the dislocation contribution in general cannot easily be separated.<sup>25</sup> More complete information might therefore be obtained through investigation of other nonlinear effects such as third-harmonic generation<sup>28</sup> or harmonic generation of transversely polarized (shear) waves.<sup>29</sup> Nonetheless, the results presented provide an example of how nonlinear ultrasonic methods can provide microstructural information beyond that available with standard (linear) ultrasonic methods.

## VI. SUMMARY

We have evaluated the nonlinear ultrasonic parameter  $\beta$  and the longitudinal phase velocity in quenched steel speci-

mens with varying carbon content. High-precision measurements showed virtually no change in the longitudinal phase velocity. Although their uncertainty was much larger, harmonic-generation experiments indicated a noticeable difference in  $\beta$  from specimen to specimen. A monotonic increase in  $\beta$  of 11% with increasing carbon content or hardness over the range 0.10–0.40 mass % C (39.0–57.5 HRC) was observed. X-ray diffraction measurements indicated the presence of extremely high numbers of dislocations in the steels. Furthermore, the dislocation density increased monotonically with carbon content. This evidence suggests that the increase in  $\beta$  with carbon content may be attributed to harmonic generation by increasing numbers of pinned dislocations affected by internal stresses. This interpretation is consistent with previous experimental and theoretical work on harmonic generation by dislocations in single crystals.

### ACKNOWLEDGMENTS

The authors thank C. M. Fortunko, W. L. Johnson, and H. M. Ledbetter for useful discussions. They appreciate the assistance of R. L. Santoyo, J. D. McColskey, B. Igarashi, and C. N. McCowan in specimen preparation.

<sup>1</sup>R. E. Green, *Treatise on Materials Science and Technology: Ultrasonic Investigation of Mechanical Properties* (Academic, New York, 1973), Vol. 3, Chap. 3.

<sup>2</sup>M. A. Breazeale and J. Philip, in *Physical Acoustics*, edited by W. P. Mason and R. N. Thurston (Academic, New York, 1984), Vol. 17, Chap. 1.

<sup>3</sup>S. Pangraz and W. Arnold, in *Review of Progress in Quantitative Nondestructive Evaluation*, edited by D. O. Thompson and D. E. Chimenti (Plenum, New York, 1994), Vol. 13, pp. 1995–2001.

<sup>4</sup>J. H. Cantrell and W. T. Yost, *J. Appl. Phys.* **81**, 2957 (1997).

<sup>5</sup>D. J. Barnard, G. E. Dace, D. K. Rehbein, and O. Buck, *J. Nondestruct. Eval.* **16**, 77 (1997).

<sup>6</sup>E. P. Papadakis, in *Physical Acoustics*, edited by W. P. Mason and R. N. Thurston (Academic, New York, 1976), Vol. 12, Chap. 5.

<sup>7</sup>M. C. Renken, S. Kim, K. W. Hollman, and C. M. Fortunko, *Proceedings of the 1997 IEEE Ultrasonics Symposium*, edited by S. C. Schneider, M. Levy, and B. R. McAvoy (IEEE, New York, 1997), pp. 483–488.

<sup>8</sup>D. C. Hurley and C. M. Fortunko, *Meas. Sci. Technol.* **8**, 634 (1997).

<sup>9</sup>A. L. Thurston, R. T. Jenkins, and H. T. O'Neil, *J. Acoust. Soc. Am.* **6**, 173 (1935).

<sup>10</sup>E. P. Papadakis, *J. Appl. Phys.* **35**, 1474 (1964).

<sup>11</sup>N. Grayeli and J. C. Shyne, in *Review of Progress in Quantitative Nondestructive Evaluation*, edited by D. O. Thompson and D. E. Chimenti (Plenum, New York, 1985), Vol. 4, pp. 927–937.

<sup>12</sup>B. E. Warren, *X-ray Diffraction* (Addison-Wesley, Reading, MA, 1969), Chap. 13.

<sup>13</sup>H. M. Rietveld, *Acta Crystallogr.* **22**, 151 (1967).

<sup>14</sup>A. C. Larson and R. B. Von Dreele, "General Structure Analysis System," Los Alamos National Laboratory Report No. LA-UR-86-748, 1988.

<sup>15</sup>D. Balzar and H. Ledbetter, *Adv. X-Ray Anal.* **38**, 397 (1995).

<sup>16</sup>J. D. Eshelby, *Solid State Phys.* **3**, 79 (1956).

<sup>17</sup>J. W. Christian, *The Theory of Transformations in Metals and Alloys* (Pergamon, London, 1965), Chaps. 6 and 7.

<sup>18</sup>J. G. M. van Berkum, Ph.D. thesis, Delft University of Technology, 1994.

<sup>19</sup>A. G. Khachaturyan, *Theory of Structural Transformations in Solids* (Wiley, New York, 1983), Chap. 6.

<sup>20</sup>G. K. Williamson and R. E. Smallman, *Philos. Mag.* **1**, 34 (1956).

<sup>21</sup>R. E. Reed-Hill, *Physical Metallurgy Principles* (Van Nostrand, New York, 1973), Chap. 18.

<sup>22</sup>P. M. Kelly and M. Kehoe, *Trans. Jpn. Inst. Met.* **17**, 399 (1976).

<sup>23</sup>A. Hikata, B. B. Chick, and C. Elbaum, *Appl. Phys. Lett.* **3**, 195 (1963).

<sup>24</sup>A. Hikata, B. B. Chick, and C. Elbaum, *J. Appl. Phys.* **36**, 229 (1965).

<sup>25</sup>A. Hikata and C. Elbaum, *Phys. Rev.* **144**, 469 (1966).

<sup>26</sup>T. Suzuki, A. Hikata, and C. Elbaum, *J. Appl. Phys.* **35**, 2761 (1964).

<sup>27</sup>A. V. Granato and K. Lücke, *J. Appl. Phys.* **27**, 583 (1956); **27**, 789 (1956).

<sup>28</sup>A. Hikata, F. A. Sewell, and C. Elbaum, *Phys. Rev.* **151**, 442 (1966).

<sup>29</sup>S. Siriwitayakorn, W. G. B. Britton, and R. W. B. Stephens, *Acustica* **56**, 247 (1984).